J|A|C|S
ARTICLES
Published on Web 01/17/2007

Vibrational Gating of Double Hydrogen Tunneling in Porphycene

Michał Gil and Jacek Waluk*

Contribution from the Institute of Physical Chemistry, Polish Academy of Sciences, Kasprzaka 44/52, 01-224 Warsaw, Poland

Received September 28, 2006; E-mail: waluk@ichf.edu.pl

Abstract: A procedure that enables determining the reaction rate from the analysis of fluorescence anisotropy is described and applied to the investigation of double hydrogen transfer between inner-cavity nitrogen atoms in electronically excited porphycene. Tautomerization proceeds as a thermally activated synchronous double hydrogen tunneling. The barrier to the reaction is dynamically modulated by a vibration that simultaneously changes the strength of two intramolecular hydrogen bonds. Different mechanisms of tautomerization in porphycene and its parent isomer, porphyrin, can be understood by analyzing the potentials for hydrogen transfer.

Introduction

Recent developments in the studies of proton/hydrogen transfer make it clear that this basic chemical reaction is a complicated, multidimensional process.[1,2] This is due to the quantum nature of the proton. The actual "transfer" can be envisaged as delocalization of the proton wave function over the region of the energy minima of the reactant and the product. The analogies to the Marcus model of electron transfer[3] are obvious, with one important quantitative difference: due to larger mass, a proton is more localized than an electron, and, therefore, its wave function decays much faster than that of an electron. Therefore, the coupling between the proton-transfer substrate and the product is extremely sensitive to the donor−acceptor distance, and the reaction rate may be modulated by vibrations that alter this distance.[2,4−6] Indeed, mode-specific hydrogen tunneling has been reported for tropolone,[7] dimers of 7-azaindole and 1-azacarbazole,[8] and complexes of 7-hydroxyquinoline with ammonia[9] or alcohol.[10] Vibrationally assisted tunneling has been proposed as the mechanism of enzyme-catalyzed reactions.[11,12] An important facet of the theory of dissipative tunneling is the possibility of an Arrhenius form of the temperature dependence of the rate, even when the process occurs exclusively through tunneling.[4,13]

For cases involving more than one proton, a question arises whether the transfer via tunneling can be realized as a synchronous process or as a sequence of single proton translocations. The systems which have been reported to exhibit multiple proton/hydrogen transfer are rare. Tunneling of four protons has been detected in calix[4]arenes;[14] the same number of hydrogen atoms participate in the translocation along an ammonia wire cluster in the excited state of 7-hydroxyquinoline·$(NH_3)_3$ complex.[9] Extensive studies have been devoted to double proton transfer in benzoic acid dimers.[15] Particularly useful models for such investigations are provided by porphyrins, where the tautomerization involves two inner-cavity hydrogen atoms. The reaction, which converts a trans tautomer into its chemically equivalent form, occurs in the ground electronic state as well as after photoexcitation. While the former process can be stopped by lowering the temperature, the latter proceeds even at 4 K.[16,17] On the basis of NMR studies of H/D isotope effects, it has now been established that the ground-state reaction starts with thermally activated tunneling of a single hydrogen atom.[18−20] This leads to a less stable cis tautomer, which upon a second hydrogen transfer step can either return to the initial or proceed to the final trans species (Figure 1).

Soon after the synthesis of porphycene (**1**, Chart 1),[21] the first constitutional isomer of porphyrin, it was realized that the

(1) Kiefer, P.; Hynes, J. In *Ultrafast Hydrogen Bond Dynamics and Proton Transfer Processes in the Condensed Phase*; Elsaesser, T., Bakker, H., Eds.; Kluwer Academic Publishers: Dordrecht, The Netherlands, 2002; p 73.
(2) Borgis, D.; Hynes, J. *J. Chem. Phys.* **1991**, *94*, 3619.
(3) Marcus, R. A.; Sutin, N. *Biochim. Biophys. Acta* **1985**, *811*, 265.
(4) Suárez, A.; Silbey, R. *J. Chem. Phys.* **1991**, *94*, 4809.
(5) Antoniu, D.; Schwartz, S. *J. Chem. Phys.* **1998**, *108*, 3620.
(6) Soudackov, A.; Hatcher, E.; Hammes-Schiffer, S. *J. Chem. Phys.* **2005**, *122*, 014505.
(7) (a) Sekiya, H.; Nagashima, Y.; Nishimura, Y. *J. Chem. Phys.* **1990**, *92*, 5761. (b) Sekiya, H.; Nagashima, Y.; Tsuji, T.; Nishimura, Y.; Mori, A.; Takeshita, H. *J. Phys. Chem.* **1991**, *95*, 10311.
(8) (a) Fuke, K.; Kaya, K. *J. Phys. Chem.* **1989**, *93*, 614. (b) Sakota, K.; Okabe, C.; Nishi, N.; Sekiya, H. *J. Phys. Chem. A* **2005**, *109*, 5245.
(9) (a) Tanner, C.; Manca, C.; Leutwyler, S. *Science* **2003**, *302*, 1736. (b) Manca, C.; Tanner, C.; Coussan, S.; Leutwyler, S. *J. Chem. Phys.* **2004**, *121*, 2578. (c) Tanner, C.; Manca, C.; Leutwyler, S. *J. Chem. Phys.* **2005**, *122*, 204326.
(10) Kwon, O. H.; Lee, Y. S.; Yoo, B. K.; Jang, D. J. *Angew. Chem., Int. Ed.* **2006**, *45*, 415.
(11) Knapp, M. J.; Klinman, J. P. *Eur. J. Biochem.* **2002**, *269*, 3113.
(12) Sutcliffe, M. J.; Scrutton, N. S. *Eur. J. Biochem.* **2002**, *269*, 3096.
(13) Antoniu, D.; Schwartz, S. *Proc. Natl. Acad. Sci. U.S.A.* **1997**, *94*, 12360.
(14) Brougham, D.; Caciuffo, R.; Horsewill, A. *Nature* **1999**, *397*, 241.
(15) Xue, Q.; Horsewill, A. J.; Johnson, M. R.; Trommsdorff, H. P. *J. Chem. Phys.* **2004**, *120*, 11107.
(16) Korotaev, O. N.; Personov, R. I. *Opt. Spectrosc. (Engl. Transl.)* **1972**, *32*, 479.
(17) Völker, S.; van der Waals, J. H. *Mol. Phys.* **1976**, *32*, 1703.
(18) Braun, J.; Limbach, H. H.; Williams, P. G.; Morimoto, H.; Wemmer, D. E. *J. Am. Chem. Soc.* **1996**, *118*, 7231.
(19) Braun, J.; Schlabach, M.; Wehrle, B.; Köcher, M.; Vogel, E.; Limbach, H. H. *J. Am. Chem. Soc.* **1994**, *116*, 6593.
(20) Schlabach, M.; Wehrle, B.; Rumpel, H.; Braun, J.; Scherer, G.; Limbach, H. H. *Ber. Bunsen-Ges. Phys. Chem.* **1992**, *96*, 821.

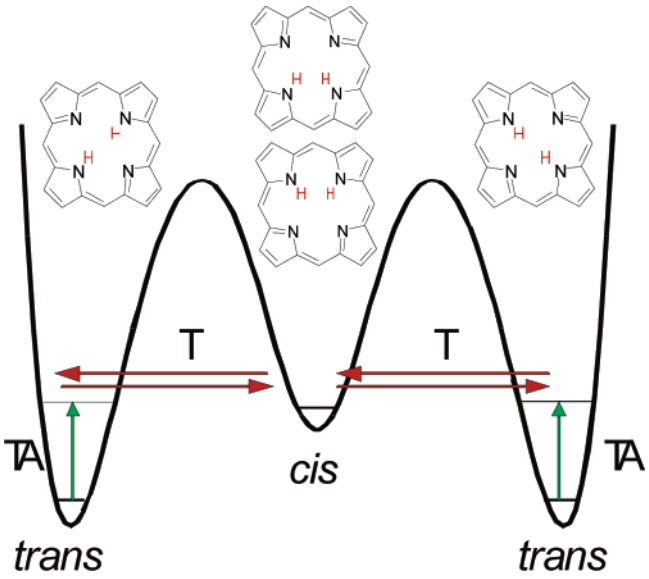

Figure 1. Tautomerization in porphyrin: TA, thermal activation, T, tunneling.

Chart 1. Trans and Cis Tautomers of the Parent Porphycene **1**, and Various Tetrasubstituted Alkyl Derivatives

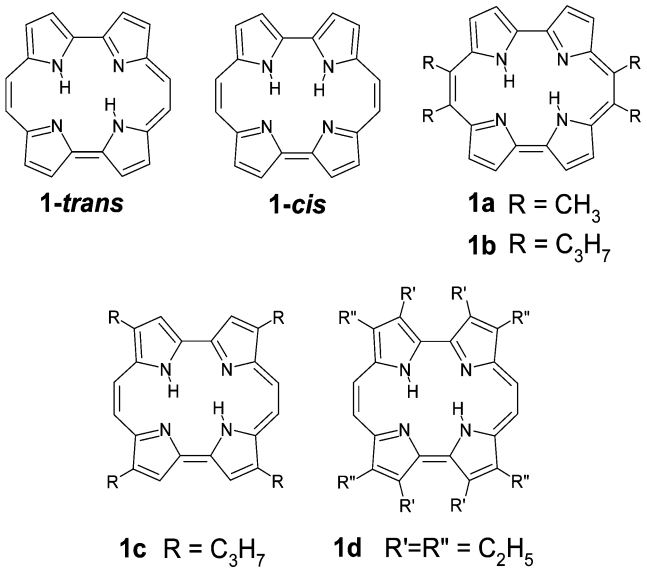

tautomeric properties of this compound are very different from those of the parent species. The motion of the internal hydrogens is too rapid to be frozen on the NMR time scale, even at 106 K.[22] In porphycene isolated in supersonic jets, doublet structure was observed in fluorescence excitation spectra;[23] this splitting was assigned to coherent double hydrogen tunneling between two trans forms in the ground electronic state. Recent studies of **1a** and **1b**, porphycenes with shorter and stronger intramolecular NH···N bonds, confirmed this picture and allowed determination of tunneling splittings in the S_0 and S_1 states.[24] Interestingly, these investigations revealed the presence of trans and cis tautomeric forms for both **1a** and **1b**, whereas no evidence was found for the presence of the cis tautomer in the parent, unsubstituted porphycene.

Contrary to the behavior of porphyrins, porphycenes reveal rapid tautomerization also in the lowest excited singlet state. The process is manifested by fluorescence depolarization in rigid media, i.e., under conditions where the molecule cannot rotate.[25−27] However, trans−trans tautomerization is equivalent to a reflection in a vertical or horizontal mirror plane perpendicular to the molecular plane. This changes the direction of the transition moment and, therefore, can lead to partially depolarized emission. The analysis of fluorescence anisotropy has shown that the trans forms of porphycene are dominant in the S_0 and S_1 states.[28]

Studies of various alkylated porphycenes demonstrated that the excited-state tautomerization rate depends crucially on the distance between the hydrogen-bonded nitrogen atoms.[28] In 9,10,19,20-tetraalkyl-substituted porphycenes **1a** and **1b**, the anisotropy measurements show that the S_1 reaction is very rapid, much shorter than the excited-state lifetime, even at 77 K. In unsubstituted porphycene **1**, as well as in the 2,7,12,17-tetrapropyl derivative **1c**, the tautomerization period becomes comparable to the S_1 lifetime (about 15 ns) around 120 K. On the other hand, in 2,3,6,7,12,13,16,17-octaethylporphycene **1d**, the process becomes too slow to compete with S_1 decay. The corresponding NH···N distances are 2.53, 2.53, 2.61, 2.63, and 2.80 Å for **1a**, **1b**, **1**, **1c**, and **1d**, respectively. The strong distance dependence of the reaction rate, spanning 4 orders of magnitude, is a sign of tunneling.

In this work, we show how the phototautomerization rate can be determined from the values of stationary fluorescence anisotropy. The methodology, briefly mentioned in previous reviews,[26,27] is described in detail and applied to porphycene embedded in various rigid environments at different temperatures. This allows us to address the questions regarding the mechanism of tautomerization in porphyrins, in particular (i) the issue of simultaneous vs stepwise transfer, (ii) the role of vibrations in promoting hydrogen transfer, and (iii) the influence of the hydrogen bond strength on the reaction parameters. The results demonstrate that photoinduced tautomerization in porphycene occurs as a concerted tunneling of two inner hydrogen atoms. The process is activated by excitation of a low-frequency mode that simultaneously reinforces both intramolecular NH···N hydrogen bonds. The mechanism of tautomerization in porphycene differs from that in the parent isomer, porphyrin, where the reaction occurs in a stepwise fashion. We explain this difference by comparing the potentials for proton migration in both molecules.

Experimental and Computational Details

Porphycene was synthesized and purified according to the procedures described earlier.[21] Spectral measurements were performed in various environments: polymer films [poly(vinyl butyral) (PVB), poly(vinyl alcohol), or polyethylene], glass-forming liquids (methanol−ethanol 1:1 v/v, propanol-1, glycerol), as well as cryogenic rare gas (argon)

(21) Vogel, E.; Köcher, M.; Schmickler, H.; Lex, J. *Angew. Chem., Int. Ed. Engl.* **1986**, *25*, 257.
(22) Wehrle, B.; Limbach, H. H.; Köcher, M.; Ermer, O.; Vogel, E. *Angew. Chem., Int. Ed. Engl.* **1987**, *26*, 934.
(23) Sepioł, J.; Stepanenko, Y.; Vdovin, A.; Mordziński, A.; Vogel, E.; Waluk, J. *Chem. Phys. Lett.* **1998**, *296*, 549.
(24) Vdovin, A.; Sepioł, J.; Urbańska, N.; Pietraszkiewicz, M.; Mordziński, A.; Waluk, J. *J. Am. Chem. Soc.* **2006**, *128*, 2577.
(25) Waluk, J.; Müller, M.; Swiderek, P.; Köcher, M.; Vogel, E.; Hohlneicher, G.; Michl, J. *J. Am. Chem. Soc.* **1991**, *113*, 5511.
(26) Waluk, J. In *Hydrogen Transfer Reactions*; Hynes, J. T., Klinman, J. P., Limbach, H. H., Schowen, R. L., Eds.; Wiley-VCH: Weinheim: 2007; Vol. 1, pp 245−271.
(27) Waluk, J. *Acc. Chem. Res.* **2006**, *39*, 945−952.
(28) Waluk, J.; Vogel, E. *J. Phys. Chem.* **1994**, *98*, 4530.

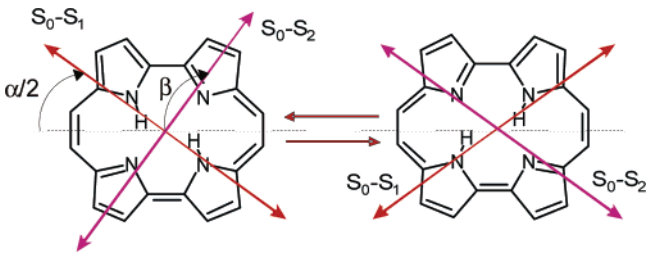

Figure 2. S_0-S_1 and S_0-S_2 transition moment directions before and after tautomerization.

and nitrogen matrices. For low-temperature studies, closed-cycle CSW-202 N (Advanced Research Systems) or Displex 202 (Air Products) helium cryostats were used.

Absorption spectra were measured on a Shimadzu UV 3100 spectrophotometer. Fluorescence spectra, fluorescence anisotropies, and decays were recorded on either an Edinburgh FS 900 CDT or a compact Jasny[29] spectrofluorimeter. To check the reliability of anisotropy measurements in polymer films, samples of perylene embedded in polyethylene were prepared. The anisotropy of fluorescence and fluorescence excitation was recorded in the temperature range 90−293 K. Fluorescence was not depolarized, even at room temperature, the anisotropy being 0.32 ± 0.02 for S_0-S_1 excitation. For the quantitative analysis of anisotropy for porphycene in polymers, only the results obtained for samples which revealed no depolarization due to the matrix were taken into account. The criterion was the anisotropy value of 0.40 ± 0.01 obtained at low temperatures (<60 K) for excitation into S_1. Quite a few samples, revealing slightly lower values, were rejected.

For time-resolved studies, IBH NanoLED laser diodes emitting at 625 and 590 nm were used as excitation sources. The decays were analyzed using iterative reconvolution procedures. While analyzing anisotropy decays, proper care was taken to use the appropriate weighing factors in the fitting procedures.

B3LYP/6-31G(d,p) calculations of optimized geometries and vibrations were performed using the Gaussian 03 suite of programs.[30]

Determination of Reaction Rates from Fluorescence Anisotropy

Due to rapid excited-state trans−trans interconversion between two chemically equivalent tautomers, fluorescence anisotropy (r) values observed for **1** embedded in a rigid environment are different from the values expected for a single emitting dipole. Instead, two transition dipoles contribute to the emission, forming an angle (α in Figure 2) which can be determined from anisotropy measurements performed under conditions when tautomerization is faster than the S_1 decay ("high-temperature" regime). The relevant formulas have been derived[26−28] and applied to porphycene studied in glassy matrices,[28] as well as to the analysis of fluorescence from single molecules of porphycene.[31] In both cases, practically the same angle between the two transition moments was obtained, 71° and 73°, respectively. When the rate of tautomerization in S_1 is much larger than that of S_1 decay, the anisotropy observed upon S_0-S_1 excitation is given by $r = [3\cos^2(\alpha) + 1]/10$.[26] For $\alpha = 72 \pm 2°$, $r = 0.13 \pm 0.01$. This value is completely different than 0.40, a value expected for only one emitting dipole with parallel transition moment in absorption and emission. The amount of fluorescence depolarization depends on α: the largest effect will be observed for $\alpha = 90°$, whereas for $\alpha = 0°$ or180° fluorescence is not depolarized by the reaction, because the directions of the transition moments in both tautomers are the same.

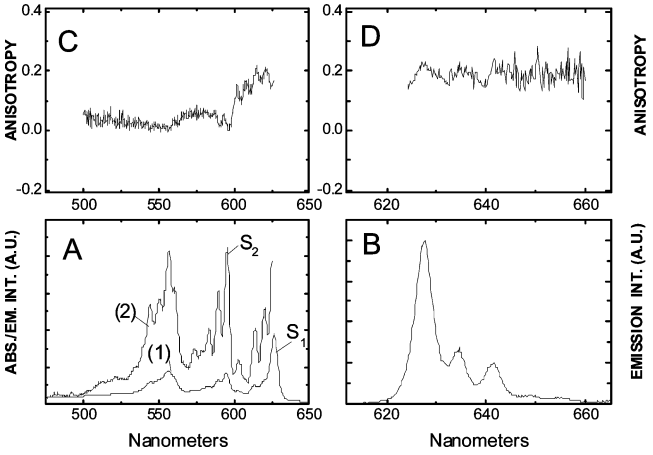

Figure 3. Results obtained for **1** in 1:1 MeOH−EtOH glass at 97 K. (A) Absorption (1) and fluorescence excitation (2), monitored at 627 nm. (B) Fluorescence. (C) Anisotropy of excitation, monitored at 628 nm. (D) Anisotropy of fluorescence excited at 614 nm.

Fluorescence depolarization due to tautomerization can also be observed when the molecule is initially excited into a higher electronic state. For instance, the S_0-S_2 transition moment in **1** is nearly orthogonal to that of the S_0-S_1 transition (Figure 2). In such case, the anisotropy value observed in the high-temperature regime will be much different than −0.20, the value expected for orthogonal absorption and emission dipoles. For $\alpha = 72 \pm 2°$, the anisotropy observed upon S_0-S_2 excitation will be 0.07 ± 0.01, using the formula[26] $r = \{3[\cos^2(\beta - \alpha/2) + \cos^2(\beta + \alpha/2)] - 2\}/10$, where β is the angle between the molecular horizontal axis and the S_0-S_2 transition moment (Figure 2).

At lower temperatures, when the rate of hydrogen transfer decreases and becomes comparable to that of S_1 decay, the anisotropies observed for S_1 and S_2 excitations become more positive and negative, respectively. Such a situation is presented in Figure 3 for **1** in a glassy 1:1 mixture of methanol−ethanol at 97 K. In the absence of excited-state tautomerization, anisotropy values of 0.40 and about −0.20 should be observed for excitation into S_1 and S_2 electronic transitions, respectively. However, the values obtained at 97 K are completely different: 0.20 ± 0.02 and 0.00 ± 0.02. Further lowering of the temperature leads to a continuous increase in the anisotropy observed for S_1 excitation and to the decrease of anisotropy obtained for S_2 excitation. Finally, at low enough temperatures, phototautomerization becomes too slow to compete with excited-state decay, and the "normal" anisotropy values of 0.40 ± 0.02 (S_1 excitation) and −0.15 ± 0.02 (S_2 excitation) are recovered. The same behavior was observed for samples of **1** embedded in polymer films (vide infra).

Information about the tautomerization rate k can, in principle, be obtained by the time-resolved anisotropy measurements. Because of the photoreaction, anisotropy changes with time. Shortly after excitation, the emission is mostly due to the initially excited tautomer. For longer delays after photoexcitation, the probability of the emission from the other tautomer increases.

(29) Jasny, J.; Waluk, J. *Rev. Sci. Instrum.* **1998**, *69*, 2242.
(30) Frisch, M. J.; et al. *Gaussian 03*, Revision B.03; Gaussian Inc.: Pittsburgh, PA, 2003.
(31) Piwoński, H.; Stupperich, C.; Hartschuh, A.; Sepioł, J.; Meixner, A.; Waluk, J. *J. Am. Chem. Soc.* **2005**, *127*, 5302.

The temporal profile of the anisotropy is given by $r(t) = {}^1/_2\,[r_1 + r_2 + (r_1 - r_2)\,e^{-2kt}]$ (see eq 9 below), where r_1 and r_2 are the (time-independent) anisotropy values for the initially excited tautomer and for the phototautomer, respectively. For excitation into S_1, the anisotropy should decay from the initial value of 0.40, while for S_0-S_2 excitation, for which the transition moment forms a large angle with the S_0-S_1 transition dipole, the initially negative value should change sign and become positive. Such behavior was indeed observed for porphycene in glycerol, organic glasses, and polymer matrices, as illustrated in Figure 4. For a detailed temperature study, however, we used a different approach that allowed determining the tautomerization rate from stationary measurements of fluorescence anisotropy.

For the derivation of equations linking anisotropy values to the photoreaction rates, we note that the anisotropy at time t after excitation is given by

$$r(t) = f_1(t)r_1 + f_2(t)r_2 = f_1(t)r_1 + (1 - f_1(t))r_2 \qquad (1)$$

r_1 and r_2 are the anisotropy values for the initially excited tautomer and for the chemically identical product of the trans−trans conversion, respectively. For excitation into S_1, $r_1 = 0.40$, and the value of r_2 is determined by the angle α, formed by the S_0-S_1 transition moments in the two tautomers (Figure 2). f_1 and f_2 are the time-dependent fractions of the two tautomers: $f_1(0) = 1$, $f_2(0) = 0$. They can be expressed using the general formulas for the reversible excited-state A*↔B* reaction, when only A is being excited:[32]

$$f_1(t) = i_1(t)/i(t); \quad f_2(t) = i_2(t)/i(t); \quad i(t) = i_1(t) + i_2(t) \qquad (2)$$

$$i_1(t) = [(k_r{}^1A_0{}^*)/(\beta_1 - \beta_2)][(X - \beta_2)\,e^{-\beta_1 t} + (\beta_1 - X)\,e^{-\beta_2 t}] \qquad (3)$$

$$i_2(t) = [(k_r{}^2k_1A_0{}^*)/(\beta_1 - \beta_2)][(e^{-\beta_2 t} - e^{-\beta_1 t})] \qquad (4)$$

$$\beta_{2,1} = {}^1/_2\,[X + Y \pm \sqrt{(Y - X)^2 + 4k_1k_{-1}}] \qquad (5)$$

$$X = k_1 + 1/\tau_1; \quad Y = k_{-1} + 1/\tau_2 \qquad (6)$$

In the above formulas, $i_{1,2}(t)$ represent the temporal profiles of the fluorescence intensity; indices 1 and 2 in the rate constants refer to the initially excited tautomer (X*) and to the photoproduct (Y*), respectively. Because we deal with a special case for which X* = Y*, these indices can be dropped. Thus k_r (the radiative constant) $= k_r{}^1 = k_r{}^2$, $k_1 = k_{-1} = k$ (the rate of excited-state tautomerization), and $\tau_1 = \tau_2 = \tau$ (fluorescence decay time). This leads to $\beta_1 = 1/\tau$ and $\beta_2 = 1/\tau + 2k$. In consequence,

$$f_1(t) = {}^1/_2\,(1 + e^{-2kt}) \qquad (7)$$

$$f_2(t) = {}^1/_2\,(1 - e^{-2kt}) \qquad (8)$$

Hence,

$$r(t) = {}^1/_2\,[r_1 + r_2 + (r_1 - r_2)\,e^{-2kt}] \qquad (9)$$

The time-averaged steady-state anisotropy r is obtained from

$$r = \int_0^\infty r(t)i(t)\,dt \,/\, \int_0^\infty i(t)\,dt \qquad (10)$$

This leads to the final expression for the reaction rate:

$$k = (1/\tau)(r_1 - r)/(2r - r_1 - r_2) \qquad (11)$$

The values of r_1 can be obtained from measurements at the low-temperature regime when the tautomerization is frozen. For S_0-S_1 excitation, r_1 should in that case be equal to 0.40. This is indeed observed (Figure 5). The values of r_2 are determined from the measurements at high temperatures, when the reaction is much faster than S_1 decay. For porphycene in PVB, we obtain $r_2 = -0.16 \pm 0.01$ ($\alpha = 75 \pm 4°$).

Both time-resolved and stationary anisotropy measurements enable the determination of tautomerization rates. The latter

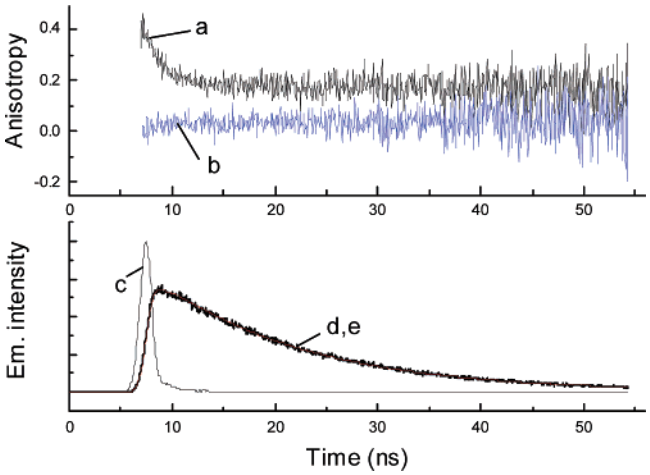

Figure 4. (Top) Decay of fluorescence anisotropy of **1** in 1:1 MeOH−EtOH glass at 97 K. Fluorescence was excited at 625 (a) and 590 nm (b). (Bottom) Excitation profile (c) and the experimental (d) and fitted (e) decay curves.

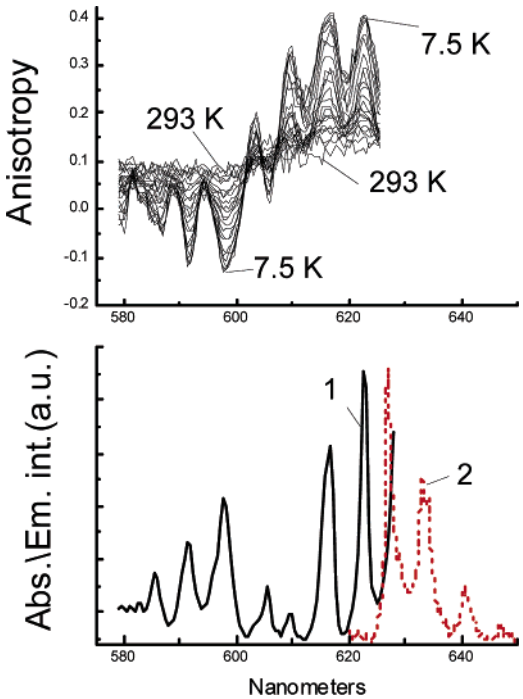

Figure 5. (Bottom) Fuorescence excitation (1) and fluorescence (2) at 15 K for **1** embedded in a poly(vinyl butyral) film. (Top) Anisotropy of fluorescence excitation, monitored at 630 nm, measured at 293 K, 250 K, 215 down to 15 K in steps of 10 K, and, finally, at 7.5 K.

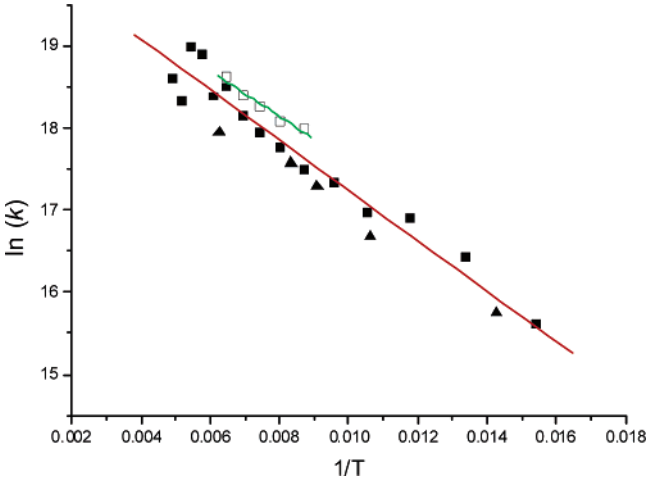

Figure 6. Arrhenius plot for the excited-state tautomerization rate in porphycene obtained for samples of **1** in PVB. Filled and empty symbols correspond to the data obtained from the analysis of anisotropy for S_0-S_1 and S_0-S_2 excitations, respectively. Squares and triangles represent the data obtained for two different samples.

technique is, however, experimentally less demanding and significantly less time-consuming.

Results and Discussion

Figure 5 shows the temperature dependence of the anisotropy of fluorescence excitation obtained for porphycene incorporated into poly(vinyl butyral) film. Three temperature regions can be distinguished: (i) At high temperature, when the reaction is much faster than the lifetime of the emitting state, the depolarization is maximal, and the anisotropy value is determined by the angle α between the S_1-S_0 transition moments in the two trans tautomers. (ii) At lower temperatures, when the rates of tautomerization and S_1 depopulation become comparable, partial depolarization is observed; in this temperature range, the rates of tautomerization can be reliably determined from the anisotropy values using eq 11. (iii) In the low-temperature regime, tautomerization becomes too slow to compete with S_1 decay; no depolarization is observed, as evidenced by r_1 values of 0.40 ± 0.01.

We consider the temperature-dependent anisotropy values for the S_0-S_1 excitation the most reliable, because these undergo larger changes than those obtained while exciting to higher-lying states; moreover, the overlap with differently polarized transitions is avoided. Still, we checked that using the anisotropy values obtained for S_0-S_2 excitation leads to similar results. Determination of the rates of tautomerization in porphycene as a function of temperature resulted in a linear Arrhenius plot (Figure 6), from which a value of the activation energy, $\Delta E = 0.55 \pm 0.05$ kcal/mol, was obtained. At first, this value looks surprisingly low compared with theoretical predictions of the barrier to tautomerization. B3LYP/6-31G(d,p) calculations predict the values of 4.1 and 6.1 kcal/mol for trans−cis transition states and trans−trans second-order saddle points (SS), respectively. Moreover, the obtained ΔE value is 4 times smaller than the computed energy difference between the cis and trans forms, 2.2 kcal mol.

The meaning of the extremely low ΔE becomes clear upon noting that its value corresponds, within the experimental error,

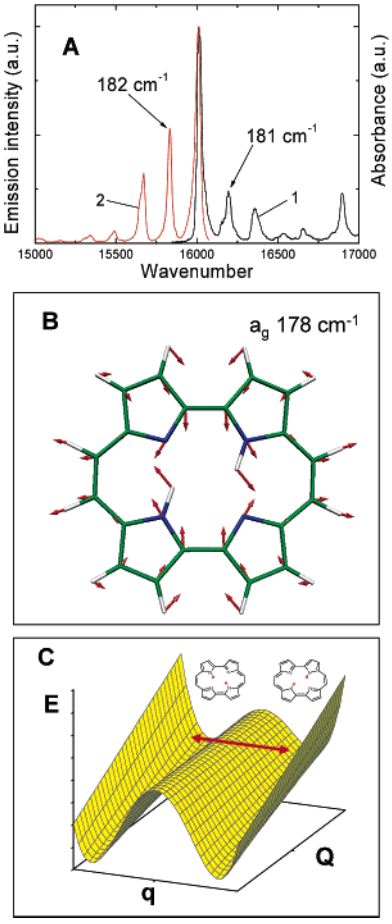

Figure 7. (A) Low-frequency mode observed in absorption (1) and emission (2) of **1** recorded in a nitrogen matrix at 15 K. (B) The form of the gating mode. (C) Coupling between the hydrogen-transfer coordinate **q** and the low-frequency mode **Q**, leading to the decrease in the tautomerization barrier. The arrow indicates the region of efficient double hydrogen tunneling.

to that of a low-frequency mode, prominent in absorption (181 cm^{-1}) and emission (182 cm^{-1}) (Figure 7A). This vibration, calculated at 178 cm^{-1}, can be safely assigned: It corresponds to in-plane distortion of the porphycene skeleton which simultaneously brings the two pairs of hydrogen-bonded nitrogen atoms closer together, at the same time making both hydrogen bonds more linear (Figure 7B). This is exactly the type of heavy-atom nuclear motion expected to modulate the hydrogen-bonding strength and, thus, the barrier to tautomerization (Figure 7C). As demonstrated earlier, variations in the NH···N distance caused by substitution lead to orders of magnitude differences in tautomerization rates.[28]

In conclusion, excited-state tautomerization in porphycene can be described as a concerted tunneling of two hydrogen atoms from a vibrationally excited level in which the reaction barrier is significantly reduced. It is important to note that the energy required for efficient tunneling is much lower than that necessary to populate the cis form. Therefore, the stepwise mechanism is less favorable.

The interpretation of the activation energy based on only one mode may, at first, look too simplistic. Porphycene has 108 vibrations, of which, in principle, many can be coupled to the tautomerization coordinate. Therefore, we have analyzed the forms of all calculated normal modes with frequencies below

(32) Birks, J. *New J. Chem.* **1977**, *1*, 453.

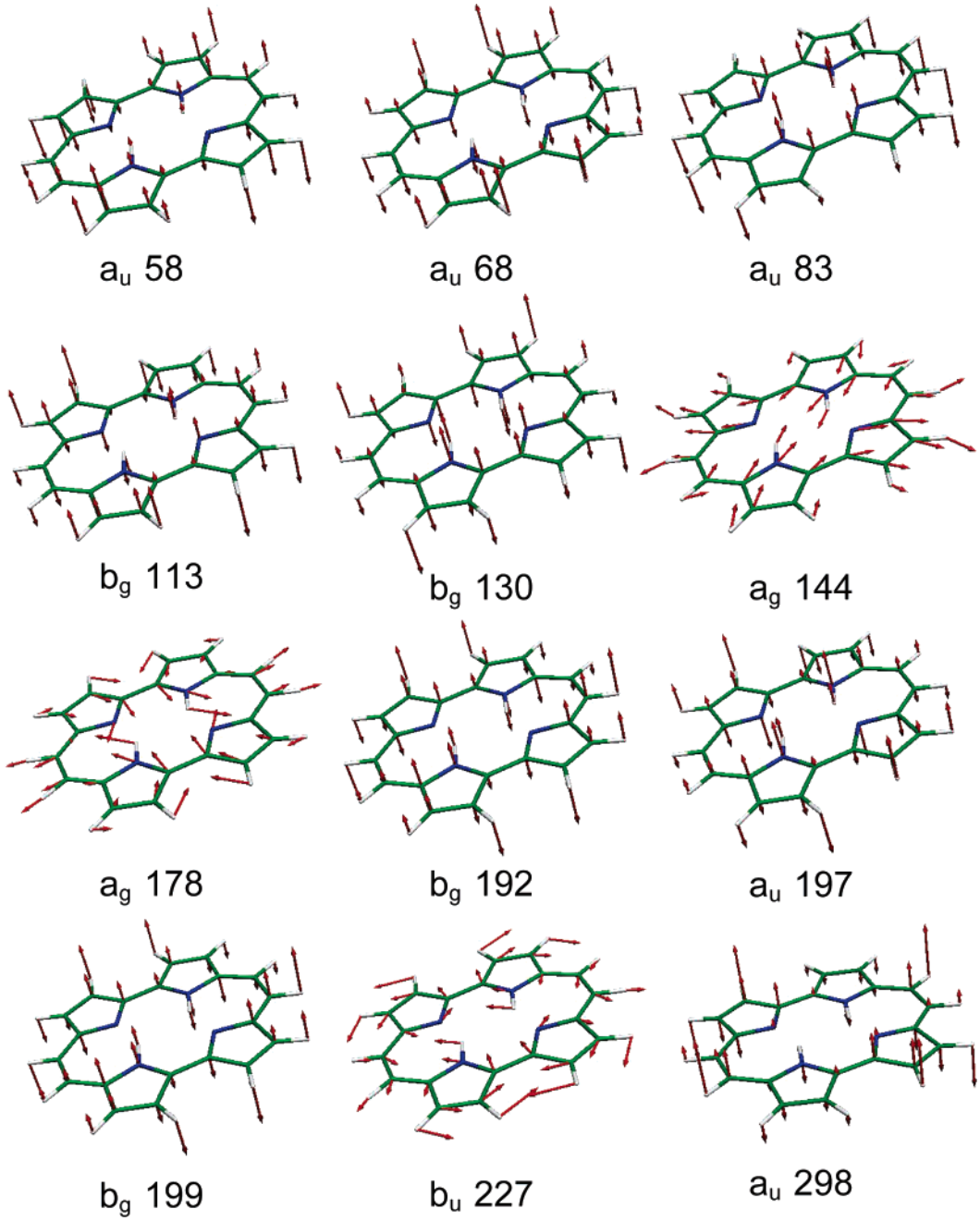

Figure 8. Shapes of the lowest energy normal modes of **1**. The calculated frequencies (cm^{-1}, scaled by 0.961) are shown next to symmetry species.

300 cm^{-1}. There are 12 such vibrations, presented in Figure 8. Nine of them correspond to out-of-plane modes, which modulate the hydrogen-bonding geometry only slightly. Due to symmetry reasons, such vibrations can only increase the N···N separation or leave it unchanged. A small increase is observed for the 197 and 298 cm^{-1} a_u modes and for the 113 cm^{-1} b_g vibration. Of the remaining three in-plane modes, two are of a_g and one of b_u symmetry. For the latter, simultaneous strengthening (or weakening) of both hydrogen bonds is impossible. Actually, the 227 cm^{-1} vibration leads to an increase of the N···N distance and should thus hinder the tautomerization. The same is observed for the 144 cm^{-1} a_g mode. Thus, in perfect agreement with experiment, the only vibration that can enhance the double hydrogen transfer is the 178 cm^{-1} a_g mode. Naturally, higher frequency vibrations can also contribute, but only at elevated temperatures. Another a_g mode that should significantly and simultaneously strengthen both hydrogen bonds is calculated (after scaling) at 955 cm^{-1}.

One of the implications of the proposed scheme is that the tunneling splitting for the gating mode should be larger than that observed for the 0−0 transition or, in general, for "neutral" vibrations, not engaged in tautomerization. Such behavior would provide a definitive evidence for the crucial role of the 180 cm^{-1} mode in promoting the tunneling. Indeed, high-resolution fluorescence spectra recorded in supersonic jets and nanohelium droplets[33] reveal for this mode a ground-state splitting of about

(33) Vdovin, A.; Waluk, J.; Dick, B.; Slenczka, A. Work in preparation.

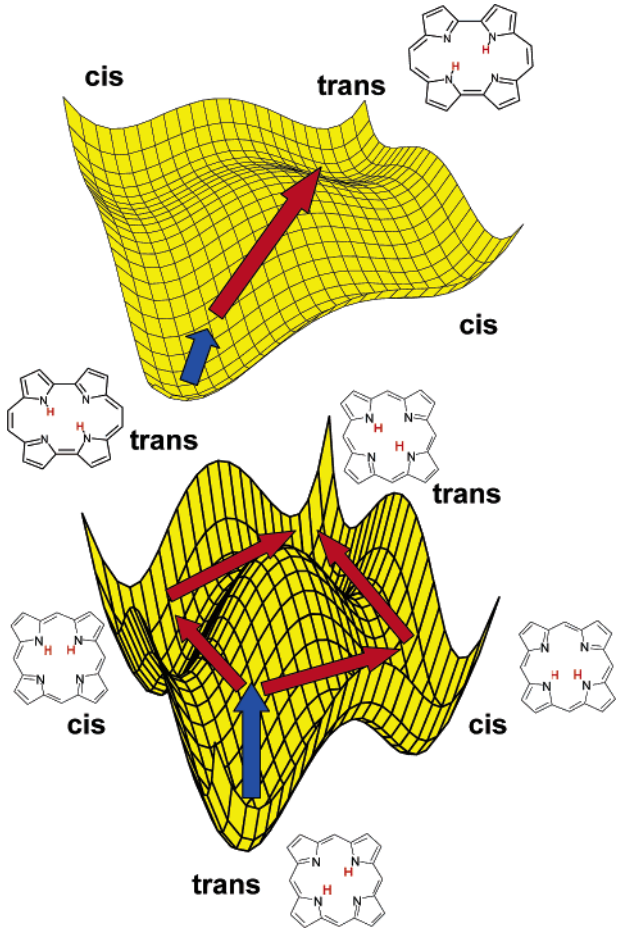

Figure 9. Preferred tautomerization paths in porphycene (top) and porphyrin (bottom). Blue arrows indicate thermal activation; red arrows indicate tunneling.

12 cm^{-1}, compared to 4.4 cm^{-1} obtained for the 0−0 transition and many other vibronic peaks. The detailed analysis of the high-resolution, low-temperature experiments will be published separately.

It should be recalled that different mechanisms are responsible for tunneling in an isolated molecule and in condensed phases. In the former, coherent tunneling leads to tunneling splitting. In the latter, tunneling becomes incoherent, and tautomerization can be described as a rate process. Moreover, in a solid environment, the two tautomers may no longer be exactly degenerate. Under such conditions, the assumption that $k_1 = k_{-1}$ may no longer hold. Equation 9 retains its general form: $r(t) = a + b\,e^{-ct}$, but the exponent c now contains not $2k$ but $k_1 + k_{-1}$, i.e., twice the arithmetic average of the forward and backward reaction rates. This effect is not expected to be large in bare **1** but may become significant for less symmetrical derivatives.

Using the above model, completely different mechanisms of tautomerization in porphyrin and porphycene can now be understood (Figure 9). For porphyrin, due to rather weak intramolecular hydrogen bonds, the barrier for trans−trans interconversion is much higher than in porphycene, and also much larger than the computed cis−trans energy difference. B3LYP/TZ2P calculations yield 24.4 and 8.3 kcal/mol for the former and latter, respectively.[34] It is not possible in porphyrin to lower the barrier to simultaneous trans−trans tautomerization below that required for a single particle trans−cis conversion. Therefore, the favorable path is that of a stepwise reaction, with trans−cis conversion as the first step.

Our findings demonstrate that it may be possible to switch between stepwise and synchronous mechanisms of proton/hydrogen translocation by controlling the strength of hydrogen bonds between the reaction partners. This result can be exploited, e.g., for the understanding of enzymatic reactions or in the design of proton wires. Our current efforts focus on inducing a synchronous double hydrogen transfer in appropriately substituted porphyrins.

Acknowledgment. This work was partially supported by the grant 3T09A 113 26 from the Polish Committee for Scientific Research.

Supporting Information Available: Complete ref 30. This material is available free of charge via the Internet at http://pubs.acs.org.

JA066976E

(34) Baker, J.; Kozlowski, P. M.; Jarzecki, A. A.; Pulay, P. *Theor. Chem. Acc.* **1997**, *97*, 59.